



HAL
open science

A multi-physics level set approach for the simulation of the hybrid Laser/GMAW process

Olivier Desmaison, Gildas Guillemot, Michel Bellet

► To cite this version:

Olivier Desmaison, Gildas Guillemot, Michel Bellet. A multi-physics level set approach for the simulation of the hybrid Laser/GMAW process. GMAW process, 10th International Seminar on Numerical Analysis of Weldability, Sep 2012, Seggau, Austria. pp.725-736. hal-00983373

HAL Id: hal-00983373

<https://minesparis-psl.hal.science/hal-00983373v1>

Submitted on 25 Apr 2014

HAL is a multi-disciplinary open access archive for the deposit and dissemination of scientific research documents, whether they are published or not. The documents may come from teaching and research institutions in France or abroad, or from public or private research centers.

L'archive ouverte pluridisciplinaire **HAL**, est destinée au dépôt et à la diffusion de documents scientifiques de niveau recherche, publiés ou non, émanant des établissements d'enseignement et de recherche français ou étrangers, des laboratoires publics ou privés.

A MULTI-PHYSIC LEVEL SET APPROACH FOR THE SIMULATION OF THE HYBRID LASER / GMAW PROCESS

O. DESMAISON*, G. GUILLEMOT*, M. BELLET*

* Mines ParisTech - Centre de Mise en Forme des Matériaux (CEMEF), CNRS UMR 7635,
Rue Claude Daunesse, BP 207, 06904 Sophia-Antipolis, France

Olivier.Desmaison@mines-paristech.fr, Gildas.Guillemot@mines-paristech.fr, Michel.Bellet@mines-paristech.fr

ABSTRACT

A new hybrid welding technique has recently been developed in order to answer to the industry needs to gather high thickness steel sheets. The combination of a laser beam and a gas metal arc enables to develop welds with a high added metal rate and low porosity. Moreover lower deformation and residual stresses are observed after cooling. Nevertheless the mastery of this technique is still in development due to the various physical phenomena which occur and interact during the welding process.

A three dimensional finite element model has been developed to simulate this welding process. Metal and air gas domains are both meshed. A Eulerian-Lagrangian approach is used in which the interface between the metal and the surrounding air or plasma is defined by a level set function. Fluid flow phenomena and temperature evolution in the weld pool are simulated.

Two moving heat sources are considered at the surface of the metal. As the arc plasma and laser beam are not modeled in the level set framework, the 'Continuum Surface Force' approach is used: a volumetric heat source distribution is applied to the immediate neighbourhood of the interface. The added metal represents an additional heat source. The Navier-Stokes equations are solved in the weld pool regarding the surface Marangoni force, the volumetric buoyancy. After solving the momentum conservation equation, metal / air interface is tracked through the resolution of a convection equation with the calculated velocity field as input.

As the hybrid welding technique is usually a multi-pass process applied on high thickness piece with high chamfer, it is of primary importance to develop a correct modeling of solid / solid contact interfaces. It is shown that the present level set approach coupled with an adaptative remeshing tool enables to follow these interfaces to simulate the entire process steps. Weld geometry on a specific steel alloy is shown and compared to the expected result.

INTRODUCTION

Welding process is largely used in the heavy industry to gather steels sheets. Recently the need to weld high thickness industrial pieces has developed. New welding conditions are needed for such pieces. For instance several passes are required in order to fill the chamfer and to develop the entire weld bead. High mechanical properties, low deformation and residual stress are expected in such process. A new hybrid welding technique has recently been proposed to answer to these needs. It combines a laser beam and a gas metal arc (Fig. 1). This hybrid laser / GMAW process enables to develop weld with a high added metal rate due to the added heat source. Moreover the final microstructure shows low defaults like porosities. This process is still in development due to the difficulties to estimate the better process parameters and to the physical phenomena interacting during the weld bead development.

A three dimensional finite element modelling is proposed to simulate this welding process. The aim of this new model is to improve the mastery of this hybrid process. A level-set approach has been developed. In a first part, this model will be presented. Its advantage for the modelling of multipasses welding will be shown. The conservation equations governing the physical phenomena are detailed. Secondly some results are presented. The first one corresponds to the full modelling. This initial result will lead to do some assumptions in the second calculation in multipasses hybrid laser / GMAW welding. This result will be detailed for various passes. The weld geometry will be discussed and compared with the expected geometry.

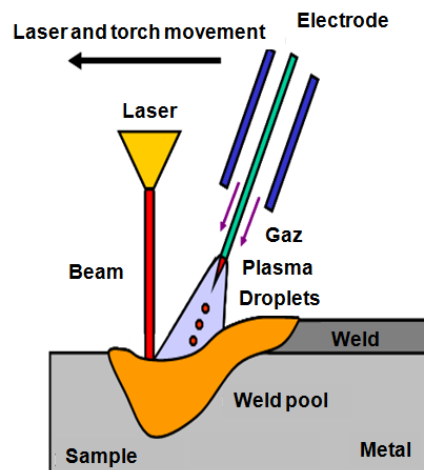


Fig. 1 : Description of the hybrid Laser – GMAW process with the various heat sources.

MODELLING

A Eulerian-Lagrangien approach is proposed to model the hybrid Laser / GMAW process. A single meshed volume is built for both metal and gas domains. A level set (LS) function is then defined corresponding to the distance, φ , from the metal / gas interface (Fig. 2). This approach enables to overcome the numerical difficulties induced by the metal / metal contacts in a multi pass welding.

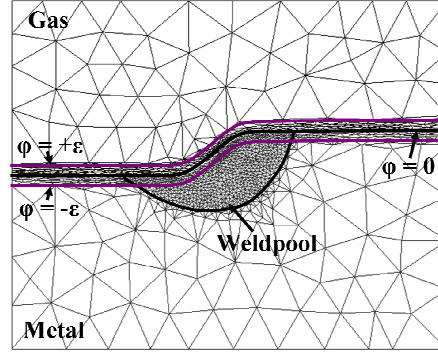


Fig. 2 : The meshed gas / metal domain and the corresponding level set function. The level set function is equal to 0 on the boundary between gas and metal (ie. $\varphi = 0$).

In this Level-Set approach, the entire materials properties are averaged using the distance function and a single mixed law corresponding to the Heaviside function (Eq. 1).

$$H(\varphi) = \frac{1}{2} \left[1 + \frac{\varphi}{\varepsilon} + \frac{1}{\pi} \sin\left(\frac{\pi\varphi}{\varepsilon}\right) \right] \quad (1)$$

Thus, any materials property α , is defined in the transition domain as an average of local gas and metal properties, α_{gas} and α_{metal} as:

$$\alpha = [1 - H(\varphi)]\alpha_{metal} + H(\varphi)\alpha_{gas} \quad (2)$$

Heat conservation equation

The temperature field evolution is calculated using the fully implicit resolution of the heat conservation equation. In non-steady state, this equation is written as:

$$\rho C_p \left(\frac{\partial T}{\partial t} + \vec{v} \cdot \vec{\nabla} T \right) - \vec{\nabla} \cdot \left(\lambda \vec{\nabla} T \right) = \dot{Q} \quad (3)$$

ρ , C_p and λ are the volume mass, the equivalent specific heat and the thermal conductivity. \mathbf{v} is the local fluid velocity and \dot{Q} is the heat source. The latent heat of transformation is taken into account following Morgan's model. Indeed the equivalent heat capacity is calculated from the enthalpy evolution as:

$$C_p^t = \frac{H^t - H^{t-dt}}{T^t - T^{t-dt}} \quad (4)$$

where t is the current time and dt is the fixed time step. The enthalpy evolution as a function of the temperature, $H(T)$, is previously calculated for a fixed solidification path model. A program has been developed using thermodynamic equilibrium calculation based on the software *Thermo-Calc (Thermocalc SA)*. The Gulliver-Scheil solidification path [6-7] has been chosen for solid fraction evolution and the corresponding enthalpy evolution has been calculated.

The volumetric heat source \dot{Q} is considered as the sum of several heat sources. The arc plasma and the defocused laser beam supply two heat sources at the metal / gas interface, \dot{Q}_p and \dot{Q}_L . These heat sources are modelled by a Gaussian distribution with specific parameters deduced from the process. Heat convection and radiation effects correspond to the third boundary condition at the metal / gas interface, \dot{Q}_T . It is noticeable that the Level Set approach does not allow imposing specific boundary conditions at the metal / gas interface. Indeed this interface is not discretized and corresponds to the continuous curve $\varphi = 0$ (ie. LS = 0) (Fig. 2) which evolves through the elements. Consequently it is not possible to impose a specific heat source as a Neumann condition on this interface. The *Continuum Surface Force* method developed by Brackbill [1] allows to transform a boundary condition into a volumetric source term [2-3]. Regarding a surface heat source \dot{Q}_S , we can integrate this source on the area of the interface S in order to obtain the total heat:

$$\int_S \dot{Q}_S d\Gamma = \int_V \dot{Q}_S \delta(\varphi) d\Omega \quad (5)$$

where V is the volume of the model and $\delta(\varphi)$ is the derivative of the Heaviside function, $H(\varphi)$ (Eq. 1). This function evolves in the domain $[-\varepsilon : +\varepsilon]$ and is equal to 0 outside this domain. This integration transforms any surface condition in volume condition. Consequently this transformation enables to impose a metal / gas interface condition in a Level-Set approach on a finite element mesh.

It should be mentioned that the average equation (2) is modified in the transition domain $[-\varepsilon : +\varepsilon]$. Indeed a shift of $-\varepsilon/4$ is introduced for the ρ , C_p and λ parameter evolution in order to prevent a sharp increase of the temperature. This phenomenon is due to high difference of these parameter between the two domains.

The impingement of molten droplets of filler metal in the weld pool corresponds to the last heat source. These droplets weld at the tip of the filler metal and fall into the liquid bath with a high velocity. Lancaster [4] has initially proposed to impose this added source, \dot{Q}_D , to the nodes included in a cylinder below the torch beam. This model has later been improved by Kumar and Bhaduri [5].

\dot{Q}_D and \dot{Q}_P correspond to the two parts of the heat source of the GMAW process, \dot{Q}_{GMAW} :

$$\dot{Q}_{GMAW} = \eta U I = \dot{Q}_P + \dot{Q}_D \quad (6)$$

where U and I are the tension and the intensity of the GMAW torch and η is the efficiency of the process. The \dot{Q}_D heat source is first estimated as a function of the temperature of droplets. The geometry of the corresponding cylinder depends of GMAW process parameters and liquid properties as detailed by Bellet and Hamide [10]. \dot{Q}_P is then estimated with the heat source \dot{Q}_{GMAW} (Eq.6). Finally, the total volumetric heat source is equal to the sum of the various sources:

$$\dot{Q} = \delta(\varphi) [\dot{Q}_P + \dot{Q}_L - \dot{Q}_T] + \dot{Q}_D \quad (7)$$

Mechanical behaviour

We propose to model the fluid flow into the weld pool during the welding process. The liquid phase velocity is computed using the Navier-Stokes equation coupled with the mass conservation equation. Two forces are considered into this equation. The buoyancy force, \vec{F}_B , is computed regarding the density evolution as a function of the temperature. The Marangoni force, \vec{F}_M , is a surface force defined as a function of the surface tension gradient:

$$\begin{cases} \vec{F}_B = \rho_0 \vec{g} [1 - \beta(T - T_0)] \\ \vec{F}_M = \frac{\partial \gamma}{\partial T} \times \frac{\partial T}{\partial \vec{s}} \end{cases} \quad (8)$$

where \vec{g} is the gravity vector, ρ_0 is the density for the temperature T_0 and β is the thermal expansion coefficient. γ is the surface tension and \vec{s} is the vector tangent to the surface. In the level-set approach, the surface Marangoni force, \vec{F}_M , is transformed in a volumetric force, $\vec{F}_{M\ vol}$, using the Continuum Surface Force method applied in the $[-\varepsilon : +\varepsilon]$ domain:

$$\vec{F}_{M\ vol} = \vec{F}_M \delta(\varphi) \quad (9)$$

Finally, the set of equations is written as:

$$\begin{cases} \rho \left(\frac{\partial \vec{v}}{\partial t} + \vec{v} \cdot \nabla \vec{v} \right) - \nabla \cdot \eta (\nabla \vec{v} + \nabla \vec{v}^T) + \nabla p = \vec{F}_B + \vec{F}_{Mvol} \\ \nabla \cdot \vec{v} = 0 \end{cases} \quad (10)$$

where \vec{v} is the liquid velocity, p is the pressure and η is the viscosity.

Surface formation

The surface evolution at the metal / gas interface is modelled with the mass conservation equation and the Navier-Stokes equation resolution regarding the gravity, \vec{F}_g , and the surface tension, \vec{F}_γ , forces. The forces \vec{F}_γ and \vec{F}_g are expressed as:

$$\begin{cases} \vec{F}_\gamma = \kappa \gamma \vec{n} \\ \vec{F}_g = \vec{g} \end{cases} \quad (11)$$

where κ is the local curvature of the interface and \vec{n} is the vector normal to the surface. Parameters κ and \vec{n} are calculated from the distance function field, ϕ :

$$\begin{cases} \kappa = -\nabla \cdot \vec{n} \\ \vec{n} = \frac{\nabla \phi}{\|\nabla \phi\|} \end{cases} \quad (12)$$

Regarding these forces, the gravity is applied on the entire liquid volume domain. The surface tension should be applied on the liquid / gas interface. In the level-set approach, this force is also transformed in a volumetric force, $\vec{F}_{\gamma vol}$, using the Continuum Surface Force method (Eq. 9). We finally solve the set of momentum and mass conservation equations as:

$$\begin{cases} \rho \left(\frac{\partial \vec{v}_\theta}{\partial t} + \vec{v}_\theta \cdot \nabla \vec{v}_\theta \right) - \nabla \cdot \eta (\nabla \vec{v}_\theta + \nabla \vec{v}_\theta^T) + \nabla p = \vec{F}_g + \vec{F}_{\gamma vol} \\ \nabla \cdot \vec{v}_\theta = \dot{\theta} \end{cases} \quad (13)$$

where $\dot{\theta}$ is the volume expansion source term. This source term corresponds to the added metal rate and is a function of the welding process parameter and metal properties (*filler metal velocity, droplets diameter, detachment frequency of the droplets ...*). The nodes influenced by this source term are the same as previously defined for the heat source \dot{Q}_D .

Thus a cylinder is estimated [10] in which an homogeneous material supply source term is introduced. \vec{v}_θ is the liquid velocity corresponding to the added metal rate. This velocity is specifically used to solve the convection equation of the level set [8] :

$$\frac{\partial \varphi}{\partial t} + \vec{v}_\theta \cdot \nabla \varphi = 0 \quad (14)$$

The new level set field enables to define the new liquid / metal interface ($\varphi = 0$) at current time regarding the added metal rate. A reinitialization method is then developed in order to respect the Eikonal property on the field φ . Indeed the norm of the distance function gradient has to be kept equal to one ($\|\nabla \varphi\| = 1$) after computation of the new distance function field. This condition is usually obtained by solving a modified convection equation coupled with the transport equation [8]. It is proposed to develop a new topological algorithm in the present model. Indeed the coupling of the modified convection equation with equations (13) has not provided valid results. The present algorithm is based on the work of Elias *et al.* [9] and is purely geometrical. The new mesh is propagated from the computed zero isovalue level set on the whole mesh step by step. An enhancement has been proposed to adapt this algorithm to heterogeneous mesh.

The resolution of (Eq. 8-13) enable to calculate both fluid flow velocity and level set position as a function of the forces that promote these fields. As presented it is proposed to separate the two resolutions. The momentum conservation equation without any added metal is first solved (Eq. 8-10) in order to estimate the fluid flow velocity. This latter velocity is then used in the heat conservation equation (Eq. 3) in the convection term.

Then the weld geometry is updated (Eq. 11-13) according to the added metal rate and surface tension force. The velocity \vec{v}_θ corresponds to the weld geometry movement and the progress of the metal / gas interface into the chamfer. Figure 3 represents the successive steps of the generalize algorithm.

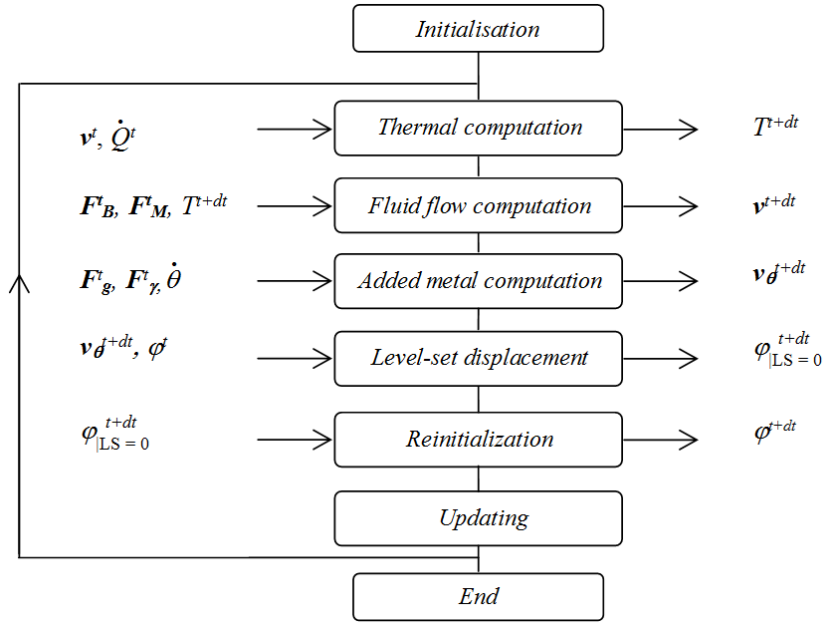


Fig. 3 : Schematic of the present algorithm proposed to model the hybrid Laser – GMAW welding process in a Level-Set approach. Superscript t and t+dt refer to the value of the fields at computation time t and t+dt.

RESULTS AND DISCUSSION

The present approach has been developed to model first the welding process on a steel sample corresponding to grade 18MnNiMo5 in a simple case to show fluid flow development. As detailed previously the material properties have been obtained from *Thermo-Calc*. The thermal conductivity in solid metal, liquid metal and gas are respectively equal to $25 \text{ W.m}^{-1}.\text{K}^{-1}$, $35 \text{ W.m}^{-1}.\text{K}^{-1}$ and $0.025 \text{ W.m}^{-1}.\text{K}^{-1}$.

Figure 4 shows the meshed domain used for the modelling of the GTAW process. The sample is a steel sheet of 15 mm thickness, 100 mm long and 50 mm wide. The total meshed domain is 20 mm height. The electrode moves in the *y* direction with a velocity of around 1 m.min^{-1} . Heat source is modelled as a moving Gaussian condition with a total power of 9500 W.

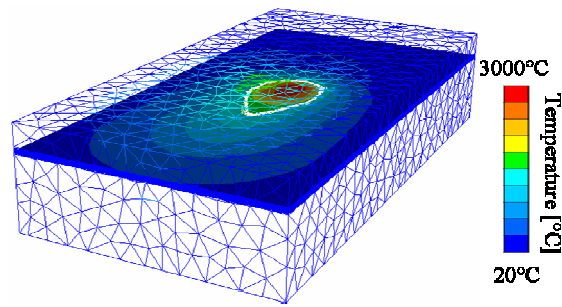


Fig. 4: Meshed domain developed to model fluid flow during the planar welding of a 18MnNiMo5 steel sheet: The temperature field is superimposed on the Level Set 0 (metal/gas interface).

Figure 5 shows the fluid flow induced in the weld pool superimposed with liquid fraction field (a-b) and temperature field (c-d). The Marangoni and buoyancy forces (Eq. 10) induce a liquid movement in the weld pool of the order of a few centimetres per second. This high velocity compared with the liquid thermal diffusivity and the small size of the weld pool corresponds to a high Peclet number into the liquid bath. Consequently the heat flow through the liquid domain is essentially due to the convection for these process parameters. It should be emphasized that a high value of the air dynamic viscosity, of 100 Pa.s is used. This value has been introduced in order to prevent shear stress at the gas/metal boundary in the weld pool. For the chosen value of the surface tension derivative (*ie.* $10^{-4} \text{ N.m}^{-1}.\text{K}^{-1}$), an inward flow is observed as shown on Fig 5 a). This flow digs the weld pool and tends to develop deeper weld beads than the one corresponding to outward flows.

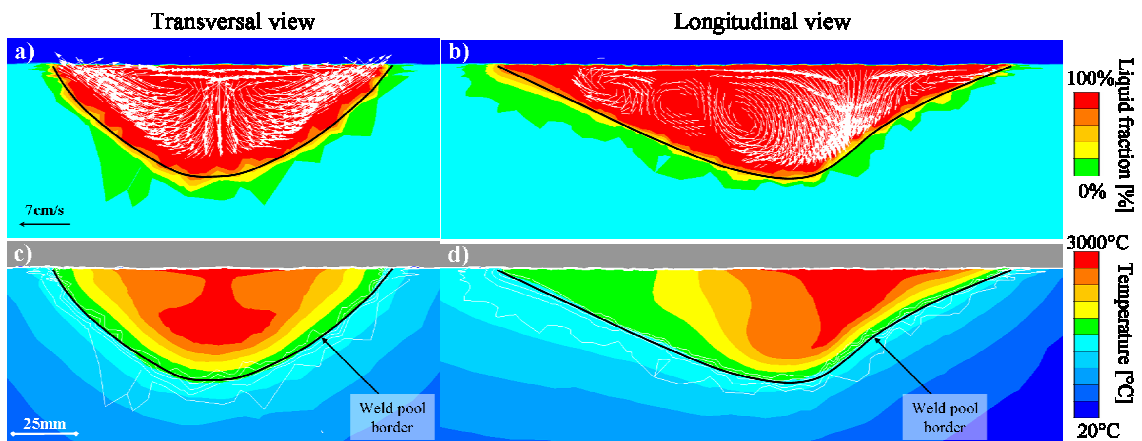


Fig. 5: a-b) Fluid flow movement during the welding of a 18MnNiMo5 steel sheet superimposed with liquid fraction field for transversal and longitudinal view. c-d) For the same time, temperature field and corresponding weld pool border.

This preliminary result leads us to model the heat conduction into the liquid domain with an enhanced value. This approach will model the liquid mixing into the weld pool and induce a decrease of the temperature gradient in this domain, comparable to the one shown in the calculations done with the momentum conservation equation resolution. In this condition, the Navier-Stokes equation resolution with mass conservation (Eq. 10) is skipped. This approach is also proposed to save time with a low influence on the temperature field in the solid domain and the weld development. It is proposed to use an enhancement factor, f_λ , of 20 as proposed by Bellet and Hamide [10] compared with the liquid conductivity.

An industrial application is then proposed corresponding to the welding of a steel sample for the same composition. The piece has a rectangular chamfer of 50 mm high and around 10 mm wide. The whole piece is 90 mm high, 120 mm long and 90 mm wide. Half of the piece is shown on Figure 6. A mesh is superimposed on the sample and a Level-Set approach is developed in order to model a multipasses process in the chamfer direction. The materials properties are constants in this second computation. Nevertheless the estimated properties [11, 12, 13] are closed to the ones computed with *Thermo-Calc*.

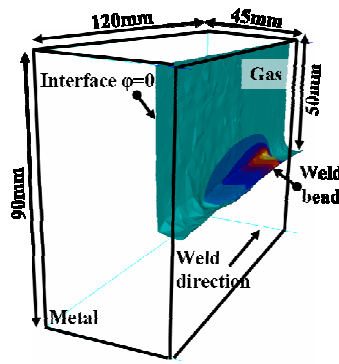


Fig. 6: Half of the piece with grade 18MnNiMo5 weld in hybrid Laser-GMAW process.

A hybrid heat source moves along the chamfer direction to develop the weld bead. The power of the laser beam is around 5000 W. This first heat source is located ahead the GMAW electrode. This latter heat source has a power of around 10 000 W and is divided in plasma and droplets heat source (Eq. 6). In this computation 30 % of its power is used for the melting of the electrode metal into droplets and 70 % for the development of the arc plasma source. Both heat sources move at the previous heat source velocity of around $1 \text{ m} \cdot \text{min}^{-1}$. The weld development is shown on figure 7 for the first pass. The liquid pool is formed ahead the weld and is progressively solidified for temperature lower than T_L . The temperature field moves with the heat sources. The temperature range is close to the expected one. A refinement of the mesh ahead the weld bead has been developed in order to catch the liquid / gas interface corresponding to the isovalue zero of the LS. Mesh is

unrefined on the walls of the chamfer which explains the rough appearance of the other surface on figure 7.

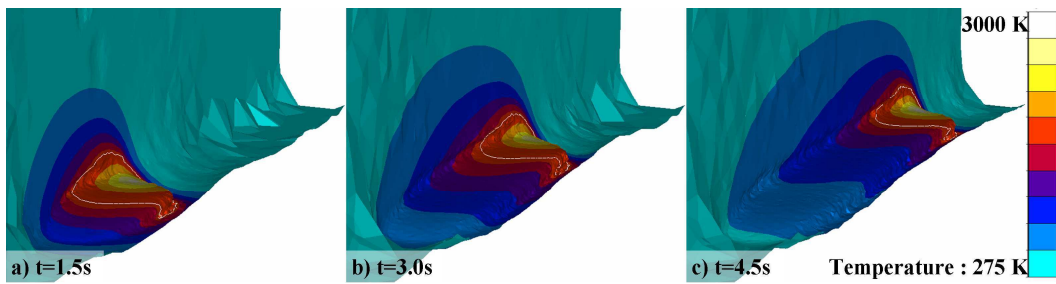


Fig. 7: Weld bead development and corresponding temperature field distribution for various time: a) 1.5s, b) 3 s, c) 4.5s. The white line corresponds to the liquidus temperature.

Three passes are then shown on figure 8 for the same time of 1.5 s. These passes correspond to the first ones that are formed at the bottom of the chamfer. Each layer corresponds to two passes. Thus a pass is developed on each side of the chamfer (*left then right*) before the next layer is formed. As it has been previously explained, the LS approach enables to manage the metal / metal contact in the multipasses welding. The overlapping of these three passes as well as the weld bead / chamfer contact is mastered.

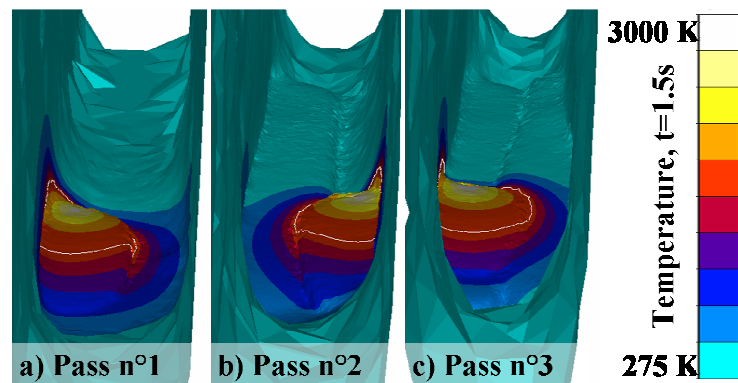


Fig. 8: The first a), second b) and third c) passes formed for the same time $t = 1.5$ s after each pass has started. The temperature field is superimposed at the weld bead surface. The white line corresponds to the liquidus temperature.

Figure 9 shows the overlapping of the same three passes in an orthogonal section. This section is closed to the experimental ones as it has been observed. The total thickness of

these passes is 4 mm which is close to the measured height on experiments. A full campaign of instrumented welding is planned in this research project in order to allow an experimental validation of temperature field and weld shape for several passes.

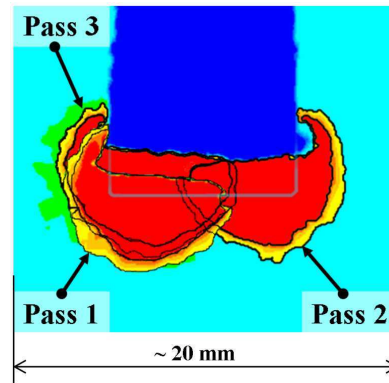


Fig. 9: Weld bead shape in an orthogonal section after three passes. The interface of each pass is shown and superimposed on the other.

CONCLUSION

A three-dimensional Level-Set approach is proposed to model the hybrid Laser / Gas Metal Arc Welding process. A large domain is considered including both initial steel sheet and the gas above the sample. This approach enables to consider the metal / metal interactions and to develop a modelling of the multipasses welding. The plasma arc heat source and droplets heat source are both considered in the GMAW heat source. The momentum conservation equation is first solved with buoyancy and Marangoni forces to calculate the liquid movement in the weld pool. This equation is then solved with the gravity and surface tension forces in order to estimate the level-Set velocity and the progress of the weld bead geometry. A continuum surface force method is used to transform surface force into volumetric force for the level-set approach. It is shown that the calculation of the liquid velocity in the weld pool can be neglected.

The efficiency of this Level-Set approach is then shown on the simulation of the welding of a steel sheet with a deep chamfer. This model enables to simulate the process with expected results for weld bead development and weld geometry. The temperature field is closed to the expected one. Future experiments will be developed in the research project to validate these results.

ACKNOWLEDGEMENTS

This work is supported by the ANR project SISHYFE (ANR-09-MAPR-0019).

REFERENCES

- [1] J.U. BRACKBILL, D.B. KOTHE, AND C. ZEMACH, A continuum method for modeling surface tension, *Journal of Computational Physics*, Vol. 100, pp. 335-354, 1991.
- [2] H. KI, J. MAZUMDER, AND P. MOHANTY, 'Modeling of laser keyhole welding: Part i. mathematical modeling, numerical methodology, role of recoil pressure, multiple reflections, and free surface evolution', *Metallurgical and Materials Transactions A*, Vol. 33, pp. 1817-1830, 2002.
- [3] H. KI, J. MAZUMDER, AND P. MOHANTY, 'Modeling of laser keyhole welding: Part ii. simulation of keyhole evolution, velocity, temperature profile, and experimental verification', *Metallurgical and Materials Transactions A*, Vol. 33, pp. 1831-1842, 2002.
- [4] J.F. LANCASTER, The physics of welding, *Physics in technology*, 15, 1984.
- [5] S. KUMAR AND S.C. BHADURI. 'Three-dimensional finite element modeling of gas metal-arc welding', *Metallurgical Transactions B*, Vol. 25, pp. 435-441, 1994.
- [6] G.H. GULLIVER, 'The quantitative effect of rapid cooling upon the constitution of binary alloys', *J. Inst. Metals*, Vol. 9, 120-157, 1913.
- [7] E. SCHEIL, 'Bemerkungen zur Schichtkristallbildung', *Zeitschrift für Metallkunde*, Vol. 34, pp. 70-72, 1942.
- [8] L. VILLE, L. SILVA, AND T. COUPEZ, Convected level set method for the numerical simulation of fluid buckling. *International Journal for Numerical Methods in Fluids*, Vol. 66, pp. 324-344, 2011.
- [9] R.N. ELIAS, M.A.D. MARTINS, AND A.L.G.A. COUTINHO, 'Simple finite element-based computation of distance functions in unstructured grids', *International journal for numerical methods in engineering*, Vol. 72, 1095-1110, 2007.
- [10] M. BELLET AND M. HAMIDE, 'Direct modelling of material deposit and identification of energy transfer in gas metal arc welding', *International Journal of Numerical Methods for Heat & Fluid Flow*, Accepted, 2012.
- [11] M. CORET, S. CALLOCH, AND A. COMBESURE, Experimental study of the phase transformation plasticity of 16mnd5 low carbon steel induced by proportional and nonproportional biaxial loading paths. *European Journal of Mechanics A/Solids*, Vol. 23, pp. 823-842, 2004.
- [12] M. CORET, S. CALLOCH, AND A. COMBESURE, 'Experimental study of the phase transformation plasticity of 16mnd5 low carbon steel under multiaxial loading. *International Journal of Plasticity*', Vol. 18, pp. 1707-1727, 2002.
- [13] Y. VINCENT, J.F. JULLIEN, AND P. GILLES, 'Thermo-mechanical consequences of phase transformations in the heat-affected zone using a cyclic uniaxial test', *International Journal of Solids and Structures*, Vol. 42, pp. 4077-4098, 2005.